academicJournals

Vol. 8(22), pp. 1228-1245, 16 June, 2013
DOI: 10.5897/IJPS2013.3879
ISSN 1992-1950 © 2013 Academic Journals
http://www.academicjournals.org/IJPS

International Journal of Physical Sciences

Full Length Research Paper

A Mode-I crack problem for two-dimensional problem of a fiber-reinforced thermoelastic with normal mode analysis

Kh. Lotfy[1] and Wafaa Hassan[2,3]*

[1]Department of Mathematics, Faculty of Science, Zagazig University, Zagazig P. O. Box 44519 Egypt.
[2]Department of Mathematics and Physics, Faculty of Engineering, Port Said Branch of Suez Canal University, Port Said, Egypt.
[3]Department of Mathematics, Faculty of Science and Arts, Al-mithnab, Qassim University, P.O. Box 931, Buridah 51931, Al-mithnab, Kingdom of Saudi Arabia.

Accepted 12 April, 2013

The aim of the present work is to investigate the influence of the Mode-I crack on the plane waves in a linearly fiber-reinforced. A general model of the equations of coupled theory (CD) and Lord-Shulman (L-S) theory with one relaxation time are applied to study the influence of reinforcement on the total deformation for an infinite space weakened by a finite linear opening Mode-I crack is solving. The material is homogeneous isotropic elastic half space. The crack is subjected to prescribed temperature and stress distribution. The normal mode analysis is used to obtain the exact expressions for the displacement components, force stresses and temperature. The variations of the considered variables with the horizontal distance are illustrated graphically. Comparisons are made with the results in two theories. A comparison also is made between the two theories for different depths.

Key words: Fiber-reinforced, Lord-Shulman theory, Mode-I crack, normal mode analysis, thermoelasticity.

INTRODUCTION

Fiber-reinforced composites are widely used in engineering structures, due to their superiority over the structural materials in applications requiring high strength and stiffness in lightweight components. A continuum model is used to explain the mechanical properties of such materials. A reinforced concrete member should be designed for all conditions of stresses that may occur and in accordance with principles of mechanics. The characteristic property of a reinforced concrete member is that its components, namely concrete and steel, act together as a single unit as long as they remain in the elastic condition that is, the two components are bounded together so that there can be no relative displacement between them. In the case of an elastic solid reinforced by a series of parallel fibers, it is usual to assume transverse isotropy. In the linear case, the associated constitutive relations, relating infinitesimal stress and strain components have five material constants. In the last three decades, the analysis of stress and deformation of fibre-reinforced composite materials has been an important research area of solid mechanics. A reinforced concrete member shall be designed for all conditions of stresses that may occur and accordance with principle of mechanics. Fiber-reinforced composites are used in a variety of structures due to their low weight and high strength. The characteristic property of a reinforced composite is that its components act together as single anisotropic units as long as they remain in the

*Corresponding author. E-mail: khlotfy_1@yahoo.com.

elastic condition. The waves propagation in a reinforced media plays a very interesting role in civil engineering and geophysics. The studies of propagation, reflection and transmission of waves are of great interest to seismologists. Such studies help them to obtain knowledge about the rock structures as well as their elastic properties and at the same time information regarding minerals and fluids present inside the earth. The idea of introducing a continuous self reinforcement at every point of an elastic solid was given by Belfield et al. (1983). The model was later applied to the rotation of a tube by Verma (1986), who has also discussed the magneto elastic shear waves in self-reinforced bodies. Singh (2002) showed that, for wave propagation in fibre-reinforced anisotropic media, this decoupling cannot be achieved by the introduction of the displacement potential. Sengupta and Nath (2001) discussed the problem of the surface waves in fibre-reinforced anisotropic elastic media. Hashin and Rosen (1964) gave the elastic moduli for fibre-reinforced materials. The problem of reflection of plane waves at the free surface of a fibre-reinforced elastic half-space was discussed by Singh and Singh (2004). Chattopadhyay and Choudhury (1990) have discussed the problem of propagation, reflection and transmission of magneto elastic shear waves in a self–reinforced medium. The reflection and transmission of plane SH wave through a self-reinforced elastic layer sandwiched between two homogeneous visco-elastic solid half-spaces has been studied by Chaudhary et al. (2004). Chattopadhyay and Choudhury (1995) studied the propagation of magneto-elastic shear waves in an infinite self-reinforced plate. Pradhan et al. (2003) studied the dispersion of Loves waves in a self-reinforced layer over an elastic non-homogenous half space. The propagation of plane waves in fibre-reinforced media is discussed by Chattopadhyay et al. (2002). The theory of couple thermo-elasticity was extended by Lord and Şhulman (1967) and Green and Lindsay (1972) by including the thermal relaxation time in constitutive relations.

Othman and Song (2007) showed the effect of initial stress, thermoelastic parameter and thermal boundary condition upon the reflection amplitude ratios. The problem of magneto-elastic transverse surfaces waves in self-reinforced elastic solid was studied by Verma et al. (1988). The problem of wave propagation in thermally conducting linear fibre-reinforced composite materials was discussed by Singh (2006).

Othman and Lotfy (2009) studied two-dimensional problem of generalized magneto-thermoelasticity under the effect of temperature dependent properties. Othman et al. (2009) studied transient disturbance in a half-space under generalized magneto-thermoelasticity with moving internal heat source. Othman and Lotfy (2010) studied the plane waves in generalized thermo -microstretch elastic half-space by using a general model of the equations of generalized thermo-microstretch for a homogeneous isotropic elastic half space. Othman and Lotfy (2009) studied the generalized thermo-microstretch elastic medium with temperature dependent properties for different theories. Othman and Lotfy (2010) studied the effect of magnetic field and inclined load in micropolar thermoelastic medium possessing cubic symmetry under three theories. The normal mode analysis was used to obtain the exact expression for the temperature distribution, thermal stresses, and the displacement components.

The investigation of interaction between a magnetic field, stress, and strain in a thermoelastic solid is very important due to its many applications in diverse field, such as geophysics (for understanding the effect of the Earth's magnetic field on seismic waves), damping of acoustic waves in a magnetic field, designing machine elements like heat exchangers, boiler tubes where the temperature induced elastic deformation occurs, biomedical engineering (problems involving thermal stress), emissions of the electromagnetic radiations from nuclear devices, development of a highly sensitive super conducting magnetometer, electrical power engineering plasma physics etc. (Lotfy, 2012a, b). The problem has been solved numerically using the normal mode analysis and many works in generalized magneto-thermo elasticity with effect of rotation and other fields can be found in (Othman and Saied, 2012a, b; 2013a, b; Othman and Atwa, 2012) for a half space fiber-reinforced. Numerical results for the conductive temperature, thermodynamic temperature, displacement components and the stresses are represented graphically and the results are analyzed.

In the recent years, considerable efforts have been devoted the study of failure and cracks in solids. This is due to the application of the latter generally in industry and particularly in the fabrication of electronic components. Most of the studies of dynamical crack problem are done using the equations of coupled or even uncoupled theories of thermoelasticity (Dhaliwal, 1980; Hasanyan et al., 2005; Ueda, 2003; Elfalaky and Abdel-Halim, 2006). This is suitable for most situations where long time effects are sought. However, when short time are important, as in many practical situations, the full system of generalized thermoelastic equations must be used (Lord and Şhulman, 1967).

In the present work we shall formulate the fiber-reinforced two-dimensional problem of thermally for an infinite space weakened by a finite linear opening Mode-I crack is solving for the considered variables. The normal mode method is used to obtain the exact expressions for the considered variables. The distributions of the considered variables are represented graphically. A comparison is carried out between the temperature, stresses and displacements as calculated from the generalized thermoelasticity L-S and coupled theories for half space fiber-reinforced in two problems. A comparison also is made between the two theories for different depths.

FORMULATION OF THE PROBLEM AND BASIC EQUATIONS

We shall consider the problem of a homogeneous, isotropic and linearly fiber-reinforced thermoelastic half-space ($x \geq 0$). The constitutive equations for a fibre-reinforced linearly elastic anisotropic medium with respect to the reinforcement direction 'a' are (Belfield et al., 1983):

$$\sigma_{ij} = \lambda e_{kk}\delta_{ij} + 2\mu_T e_{ij} + \alpha(a_k a_m e_{km}\delta ij + a_i a_j e_{kk}) + 2(\mu_L - \mu_T)(a_i a_k e_{kj} + a_j a_k e_{ki}) + \beta a_k a_m e_{km} a_i a_j - \gamma(T - T_0)\delta_{ij}. \quad (1)$$

Where σ_{ij} are components of stress; e_{ij} are the components of strain; λ, μ_T are elastic constants; $\alpha, \beta, (\mu_L - \mu_T)$ are reinforcement parameters, $\gamma = (3\lambda + 2\mu)\alpha_t$, α_t thermal expansion coefficient and $\underline{a} \equiv (a_1, a_2, a_3), \quad a_1^2 + a_2^2 + a_3^2 = 1.$ We choose the fiber-direction as $\underline{a} \equiv (1,0,0).$ The strains can be expressed in terms of the displacement u_i as:

$$e_{ij} = \frac{1}{2}(u_{i,j} + u_{j,i}). \quad (2)$$

For plane strain deformation in the xy-plane [displacement $\underline{u} = (u, v, 0)$] $\frac{\partial}{\partial z} = 0$, $w = 0$ .Equation (1) then yields

$$\sigma_{xx} = A_{11}u_{,x} + A_{12}v_{,y} - \gamma(T - T_0), \quad (3)$$

$$\sigma_{yy} = A_{22}v_{,y} + A_{12}u_{,x} - \gamma(T - T_0), \quad (4)$$

$$\sigma_{zz} = A_{12}u_{,x} + \lambda v_{,y} - \gamma(T - T_0), \quad (5)$$

$$\sigma_{xy} = \mu_L(u_{,y} + v_{,x}), \qquad \sigma_{zx} = \sigma_{zy} = 0. \quad (6)$$

Where

$$A_{11} = \lambda + 2(\alpha + \mu_T) + 4(\mu_L - \mu_T) + \beta, \qquad A_{12} = \alpha + \lambda,$$
$$A_{22} = \lambda + 2\mu_T. \quad (7)$$

The equation of motion in a rotating frame of reference in the context of Lord-Shulman's(LS) theory is

$$\rho\ddot{u}_i = \sigma_{ij,j}, \quad (i, j = 1,2,3). \quad (8)$$

The heat conduction equation

$$kT_{,ii} = \left(\frac{\partial}{\partial t} + \tau_0 \frac{\partial^2}{\partial t^2}\right)(\rho C_E T + \gamma T_0 u_{i,i}). \quad (9)$$

Where ρ is the density, k is the thermal conductivity, C_E is specific heat at constant strain and T is temperature above reference temperature T_0.

Using the summation convection. From Equations (3) to (6), we note that the third equation of motion in Equation (8) identically satisfied and first two equations become:

$$\rho\left(\frac{\partial^2 u}{\partial t^2}\right) = A_{11}\frac{\partial^2 u}{\partial x^2} + B_2\frac{\partial^2 v}{\partial x \partial y} + B_1\frac{\partial^2 u}{\partial y^2} - \gamma\frac{\partial T}{\partial x}, \quad (10)$$

$$\rho\left(\frac{\partial^2 v}{\partial t^2}\right) = A_{22}\frac{\partial^2 v}{\partial y^2} + B_2\frac{\partial^2 u}{\partial x \partial y} + B_1\frac{\partial^2 v}{\partial x^2} - \gamma\frac{\partial T}{\partial y}. \quad (11)$$

Where $B_1 = \mu_L, \qquad B_2 = \alpha + \lambda + \mu_L.$

For convenience, the following non-dimensional variables are used:

$$x' = c_1\eta x, \quad y' = c_1\eta y, \quad u' = c_1\eta u, \quad v' = c_1\eta v, \quad t' = c_1^2\eta t, \quad \tau_0' = c_1^2\eta\tau_0,$$
$$\Omega' = \frac{\Omega}{c_1^2\eta}, \quad \theta = \gamma\frac{(T - T_0)}{\lambda + 2\mu_T}, \quad \sigma_{ij}' = \frac{\sigma_{ij}}{\mu_T}. \quad i, j = 1,2. \quad (12)$$

Where $\eta = \frac{\rho C_E}{k}, \qquad c_1^2 = \frac{\lambda + 2\mu_T}{\rho}.$

In terms of non-dimensional quantities defined in Equation (12), the above governing equations reduce to (dropping the dashed for convenience)

$$\frac{\partial^2 u}{\partial t^2} = h_{11}\frac{\partial^2 u}{\partial x^2} + h_2\frac{\partial^2 v}{\partial x \partial y} + h_1\frac{\partial^2 u}{\partial y^2} - \frac{\partial \theta}{\partial x}, \quad (13)$$

$$\frac{\partial^2 v}{\partial t^2} = h_{22}\frac{\partial^2 v}{\partial y^2} + h_2\frac{\partial^2 u}{\partial x \partial y} + h_1\frac{\partial^2 v}{\partial x^2} - \frac{\partial \theta}{\partial y}, \quad (14)$$

$$\frac{\partial^2 \theta}{\partial x^2} + \frac{\partial^2 \theta}{\partial y^2} = \left(\frac{\partial}{\partial t} + \tau_0\frac{\partial^2}{\partial t^2}\right)\left(\theta + \varepsilon\left(\frac{\partial u}{\partial x} + \frac{\partial v}{\partial y}\right)\right). \quad (15)$$

Where

$$(h_{11}, h_{22}, h_1, h_2) = \frac{(A_{11}, A_{22}, B_1, B_2)}{(\lambda + 2\mu_T)}, \qquad \varepsilon = \frac{\gamma^2 T_0}{\rho C_E(\lambda + 2\mu_T)}.$$
$$\mu_T\sigma_{xx} = A_{11}u_{,x} + A_{12}v_{,y} - (\lambda + 2\mu_T)\theta, \quad (16)$$

$$\mu_T\sigma_{yy} = A_{22}v_{,y} + A_{12}u_{,x} - (\lambda + 2\mu_T)\theta, \quad (17)$$

$$\mu_T\sigma_{zz} = A_{12}u_{,x} + \lambda v_{,y} - (\lambda + 2\mu_T)\theta, \quad (18)$$

$$\mu_T\sigma_{xy} = \mu_L(u_{,y} + v_{,x}), \qquad \sigma_{zx} = \sigma_{zy} = 0. \quad (19)$$

NORMAL MODE ANALYSIS

The normal mode analysis gives exact solutions without any assumed restrictions on temperature, displacement and stress distributions. It is applied to a wide range of problems in different branches. It can be applied to boundary-layer problems, which are described by the linearized Navier-Stokes equations in electro hydrodynamics. The normal mode analysis is, in fact, to look for the solution in Fourier transformed domain. Assuming that all the field quantities are sufficiently smooth on the real line such that normal mode analysis of these functions exists. The solution of the considered physical variable can be decomposed in terms of normal modes as the following form:

$$[u,v,\theta,\sigma_{ij}](x,y,t)=[u^*(x),v^*(x),\theta^*(x),\sigma^*_{ij}(x)]\exp(\omega t+iay). \tag{20}$$

Where ω is the (complex) time constant. $i=\sqrt{-1}$, a is the wave number in the $y-$ direction and $u^*(x),v^*(x),\theta^*(x)$ and $\sigma^*_{ij}(x)$ are the amplitude of the field quantities. Using Equation (20), then Equations (13) to (19) take the form

$$[h_{11}D^2-A_1]u^*+[iah_2D]v^*=D\theta^*, \tag{21}$$

$$[h_1D^2-A_2]v^*+[iah_2D]u^*=ia\theta^*, \tag{22}$$

$$A_4Du^*+iaA_4]v^*=[D^2-A_3]\theta^*, \tag{23}$$

$$\mu_T\sigma^*_{xx}=A_{11}Du^*+iaA_{12}v^*-(\lambda+2\mu_T)\theta^*, \tag{24}$$

$$\mu_T\sigma^*_{yy}=A_{12}Du^*+iaA_{22}v^*+-(\lambda+2\mu_T)\theta^*, \tag{25}$$

$$\mu_T\sigma^*_{zz}=A_{12}Du^*+ia\lambda v^*-(\lambda+2\mu_T)\theta^*, \tag{26}$$

$$\mu_T\sigma^*_{xy}=\mu_L(iau^*+Dv^*), \qquad \sigma^*_{zx}=\sigma^*_{zy}=0. \tag{27}$$

Where

$$A_1=\omega^2+h_1a^2, \qquad A_2=\omega^2+h_{22}a^2,$$

$$A_3=a^2+\omega+\omega^2\tau_0, \qquad A_4=\omega\varepsilon+\varepsilon\omega^2\tau_0, \qquad D=\frac{d}{dx}$$

Eliminating $\theta^*(x)$ and $v^*(x)$ between Equations (21) to (23), we obtain the ordinary differential equation satisfied by $u^*(x)$.

$$[D^6-AD^4+BD^2-C]u^*(x)=0. \tag{28}$$

where

$$A=\frac{1}{h_1h_{11}}\{h_{11}A_2+h_1A_1+h_1A_4+h_1h_{11}A_3-h_2^2a^2\}, \tag{29}$$

$$B=\frac{1}{h_1h_{11}}\{A_1A_2+h_{11}A_2A_3+h_1A_1A_3+h_{11}a^2A_4+A_2A_4-h_2^2a^2A_3-2h_2a^2A_4\}, \tag{30}$$

$$C=\frac{1}{h_1h_{11}}\{A_1A_2A_3+A_1A_4a^2\}. \tag{31}$$

In a similar manner, we get

$$[D^6-AD^4+BD^2-C]\{v^*(x),\theta^*(x)\}=0. \tag{32}$$

The above equation can be factorized as

$$(D^2-k_1^2)(D^2-k_2^2)(D^2-k_3^2)u^*(x)=0, \tag{33}$$

where, $k_n^2\,(n=1,2,3)$ are the roots of the following characteristic equation

$$k^6-Ak^4+Bk^2-C=0.. \tag{34}$$

The solution of Equation (33) which is bounded as $x\to\infty$, is given by

$$u^*(x)=\sum_{n=1}^{3}M_n(a,\omega)\exp(-k_nx) \tag{35}$$

Similarly

$$v^*(x)=\sum_{n=1}^{3}M'_n(a,\omega)\exp(-k_nx) \tag{36}$$

$$\theta^*(x)=\sum_{n=1}^{3}M''_n(a,\omega)\exp(-k_nx) \tag{37}$$

Where M_n, M'_n and M''_n are some parameters depending on a and ω.

Substituting from Equations (35) to (37) into Equations (21) to (23), we have

$$M'_n(a,\omega)=H_{1n}M_n(a,\omega), \qquad n=1,2,3. \tag{38}$$

$$M''_n(a,\omega)=H_{2n}M_n(a,\omega), \qquad n=1,2,3. \tag{39}$$

Where

$$H_{1n}=\frac{-iah_{11}k_n^2+iaA_1+iah_2k_n^2}{h_2k_na^2+h_1k_n^3-A_2k_n}, \qquad n=1,2,3. \tag{40}$$

$$H_{2n}=\frac{-A_4k_n+iaA_4H_{1n}}{k_n^2-A_3}, \qquad n=1,2,3. \tag{41}$$

Thus, we have

$$v^*(x) = \sum_{n=1}^{3} H_{1n} M_n(a,\omega)\exp(-k_n x) \tag{42}$$

$$\theta^*(x) = \sum_{n=1}^{3} H_{2n} M_n(a,\omega)\exp(-k_n x) \tag{43}$$

Substitution of Equations (35), (42) and (43) into Equations (24) to(27), we get

$$\mu_T \sigma_{xx}^* = \sum_{n=1}^{3} H_{3n} M_n(a,\omega)\exp(-k_n x), \tag{44}$$

$$\mu_T \sigma_{yy}^* = \sum_{n=1}^{3} H_{4n} M_n(a,\omega)\exp(-k_n x), \tag{45}$$

$$\mu_T \sigma_{zz}^* = \sum_{n=1}^{3} H_{5n} M_n(a,\omega)\exp(-k_n x), \tag{46}$$

$$\mu_T \sigma_{xy}^* = \sum_{n=1}^{3} H_{6n} M_n(a,\omega)\exp(-k_n x), \tag{47}$$

where

$$H_{3n} = -A_{11}k_n + iaA_{12}H_{1n} - (\lambda + 2\mu_T)H_{2n} \qquad n = 1,2,3. \tag{48}$$

$$H_{4n} = -A_{12}k_n + iaA_{22}H_{1n} - (\lambda + 2\mu_T)H_{2n} \qquad n = 1,2,3. \tag{49}$$

$$H_{5n} = -A_{12}k_n + ia\lambda H_{1n} - (\lambda + 2\mu_T)H_{2n} \qquad n = 1,2,3. \tag{50}$$

$$H_{6n} = \mu_L(ia - k_n H_{1n}) \qquad n = 1,2,3. \tag{51}$$

The normal mode analysis is, in fact, to look for the solution in Fourier transformed domain. Assuming that all the field quantities are sufficiently smooth on the real line such that normal mode analysis of these functions exists.

APPLICATION

Problem 1 (A Mode-I crack)

The plane boundary subjects to an instantaneous normal point force and the boundary surface is isothermal, the boundary conditions (Figure 1) at the vertical plan $y = 0$ and in the beginning of the crack at $x = 0$ are

$$\sigma_{yy}(x,y,t) = -p(y,t), \quad |x| < a \tag{52}$$

$$\theta(x,y,t) = f(y,t) \qquad |x| < a \text{ and } \frac{\partial\theta}{\partial y} = 0 \qquad |x| > a \tag{53}$$

$$\sigma_{xy}(x,y,t) = 0 \qquad -\infty < x < \infty \tag{54}$$

Substituting the expressions of the variables considered into the above boundary conditions, we get

$$\sum_{n=1}^{3} H_{3n} M_n(a,\omega) = -p^*(y,t) \tag{55}$$

$$\sum_{n=1}^{3} H_{2n} M_n(a,\omega) = f^*(y,t) \tag{56}$$

$$\sum_{n=1}^{3} H_{6n} M_n(a,\omega) = 0 \tag{57}$$

Invoking the boundary conditions (55) to (57) at the surface $x = 0$ of the plate, we obtain a system of three equations. After applying the inverse of matrix method, we have the values of the three constants $M_j,\ j = 1,2,3$. Hence, we obtain the expressions of displacements, temperature distribution and another physical quantities of the plate the muscles.

$$\begin{pmatrix} M_1 \\ M_2 \\ M_3 \end{pmatrix} = \begin{pmatrix} H_{41} & H_{42} & H_{43} \\ H_{21} & H_{22} & H_{23} \\ H_{61} & H_{62} & H_{63} \end{pmatrix}^{-1} \begin{pmatrix} -p^* \\ f^* \\ 0 \end{pmatrix} \tag{58}$$

Problem 2

A time-dependent heat punches across the surface of semi-infinite thermo-elastic half space. In the physical problem, we should suppress the positive exponential that are unbounded at infinity. The constants $M_1, M_2 \text{ and } M_3$ have to be chosen such that the boundary conditions on the surface x = 0 take the form

(1) Thermal boundary condition that the surface of the half-space subjected to a

$$\theta(0,y,t) = 0 \quad \text{on} \quad x = 0, \tag{59}$$

(2) Thermal boundary condition that the surface of the half-space subjected to a

$$\sigma_{xx}(0,y,t) = -p_1(y,t) \quad \text{on} \quad x = 0, \tag{60}$$

$$\sigma_{xy}(0,y,t) = 0 \quad \text{on} \quad x = 0. \tag{61}$$

where p is given function of y and t. Invoking the boundary conditions (59 to 61) at the surface $x = 0$ of the plate, we obtain a system of three equations. After applying the inverse of matrix method, we have the values of the three constants $M_j,\ j = 1,2,3$.

$$\begin{pmatrix} M_1 \\ M_2 \\ M_3 \end{pmatrix} = \begin{pmatrix} H_{31} & H_{32} & H_{33} \\ H_{21} & H_{22} & H_{23} \\ H_{61} & H_{62} & H_{63} \end{pmatrix}^{-1} \begin{pmatrix} 0 \\ -p_1 \\ 0 \end{pmatrix} \tag{62}$$

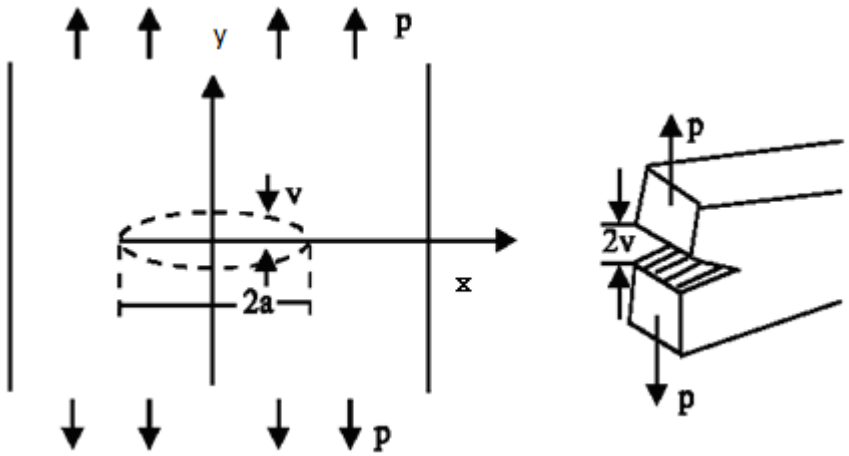

Figure 1. Displacement of an external Mode-I crack.

From this matrix we obtain the values of the three constants M_1, M_2 and M_3. Hence, we obtain the expressions of displacements, force stress, coupled stress and temperature distribution for generalized thermoelastic medium.

NUMERICAL RESULTS

In order to illustrate the theoretical results obtained in preceding section, to compare these in the context of various theories of thermoelasticity and reinforcement on wave propagation. We now present some numerical results for the physical constants. We now present some numerical results for the physical constants (Singh and Singh, 2004).

$\lambda = 7.59\text{x}10^9\ N/m^2$, $\mu_T = 1.89\text{x}10^9\ N/m^2$, $\mu_L = 2.45\text{x}10^9\ N/m^2$,
$\alpha = -1.28\text{x}10^9\ N/m^2$, $\beta = 0.32\text{x}10^9\ N/m^2$, $\rho = 7800 kg/m^2$,
$\alpha_t = 1.78\ \text{x}10^{-5}\ N/m^2$, $k = 386$, $C_E = 383.1$, $\tau_0 = 0.02$,
$a = 1$
$T_0 = 293\text{k}$ $f^* = 1$, $p^* = 2$, $\omega = \omega_0 + i\xi$ $\omega_0 = 2$,
$\xi = 1$
$C_E = 383.1$ $J/(kgk)$, $\mu = 3.86\times10^{10}$ kg/ms^2

The computations were carried out for a value of time $t = 0.1$. The numerical technique, outlined above, was used for the distribution of the real part of the thermal temperature θ, the displacement u and v, the stresses σ_{xx}, σ_{yy}, σ_{zz} and σ_{xy} distribution for the problem. The field quantities, temperature, displacement components u, v and stress components σ_{xx}, σ_{yy}, σ_{zz} and σ_{xy} depend not only on space x and time t but also on the thermal relaxation time τ_0. Here all the variables are taken in non dimensional forms.

The results are shown in Figures 1 to 14. The graph shows the two curves predicted by different theories of thermoelasticity. In these figures, the solid lines represent the solution in the coupled theory; the dashed lines represent the solution in the generalized Lord and Shulman theory. We notice that the results for the temperature, the displacement and stresses distribution when the relaxation time is including in the heat equation are distinctly different from those when the relaxation time is not mentioned in heat equation, because the thermal waves in the Fourier's theory of heat equation travel with an infinite speed of propagation as opposed to finite speed in the non-Fourier case. This demonstrates clearly the difference between the coupled and the theory of thermoelasticity (LS).

Problem 1

For the value of y, namely y = -1, were substituted in performing the computation. It should be noted (Figure 2) that in this problem I, the crack's size, x is taken to be the length in this problem so that $0 \le x \le 1.2$, $y = 0$ represents the plane of the crack that is symmetric with respect to the y -plane. It is clear from the graph that θ has a maximum value at the beginning of the crack ($x = 0$), it begins to fall just near the crack edge ($\text{x} \approx 1.2$), where it experiences sharp decreases (with a maximum negative gradient at the crack's end). The value of temperature quantity converges to zero with increasing the distance x.

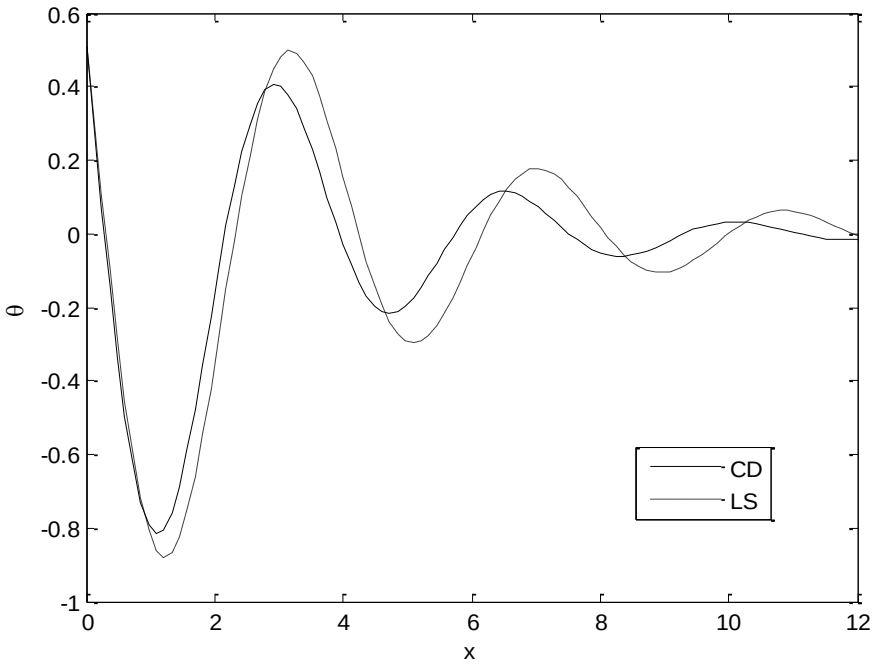

Figure 2. The temperature distribution for problem 1.

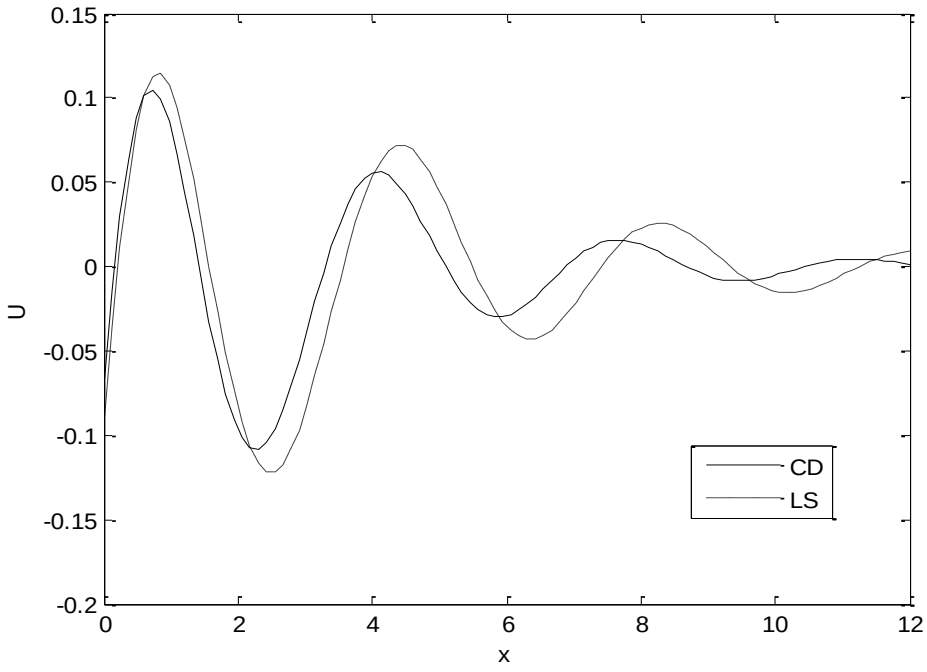

Figure 3. Horizontal displacement distribution u for problem 1.

Figure 3 the horizontal displacement, u begins with increases near the crack edge ($x \approx 1.2$), then smooth decreases again to reach its minimum magnitude just at the crack end. Beyond it u falls again to try to retain zero at infinity. Figure 4, the vertical displacement V, we see that the displacement component V always starts from the negative value and terminates at the zero value. Also, at the crack end to reach minimum value, beyond

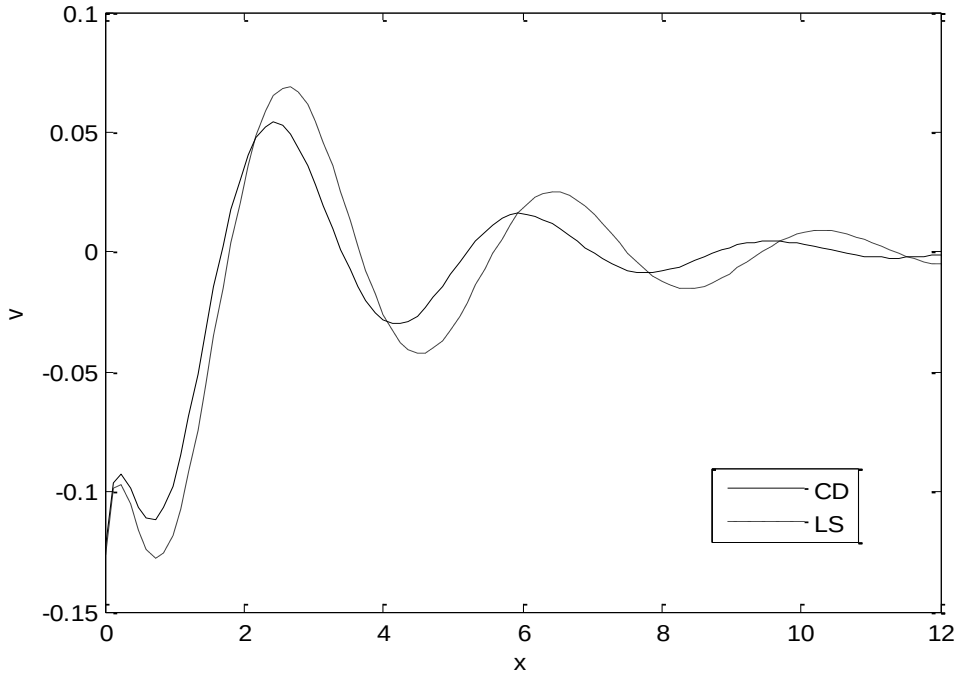

Figure 4. Vertical displacement distribution v for problem 1.

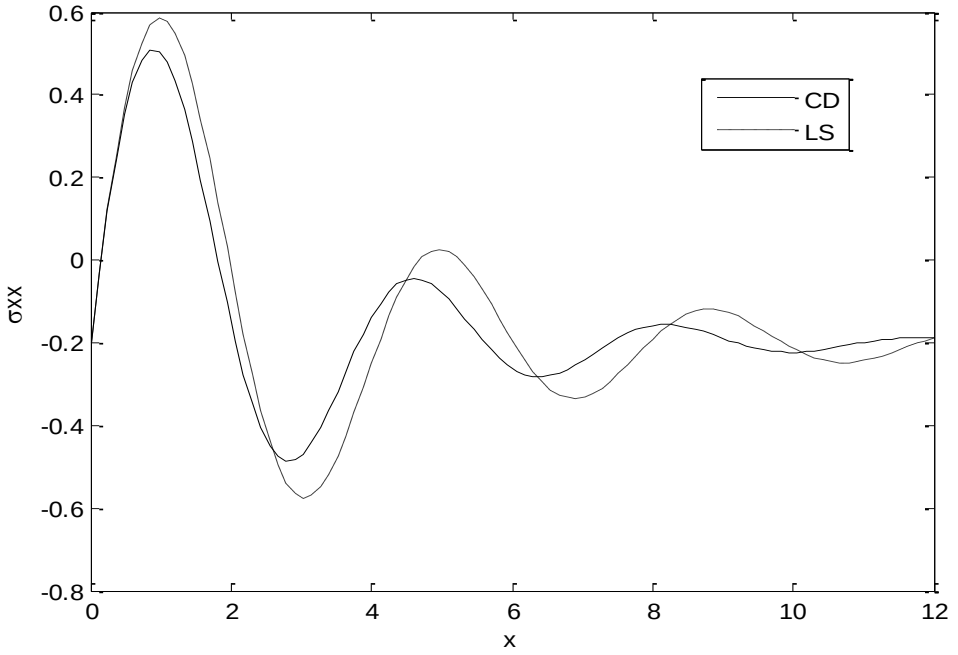

Figure 5. The distribution of stress component σ_{xx} for problem 1.

reaching zero at the three double of the crack size (state of particles equilibrium). The displacements u and v show different behaviours, because of the elasticity of the solid tends to resist vertical displacements in the problem under investigation. Both of the components show different behaviours, the former tends to increase to maximum just before the end of the crack. Then it falls to a minimum with a highly negative gradient. Afterwards it

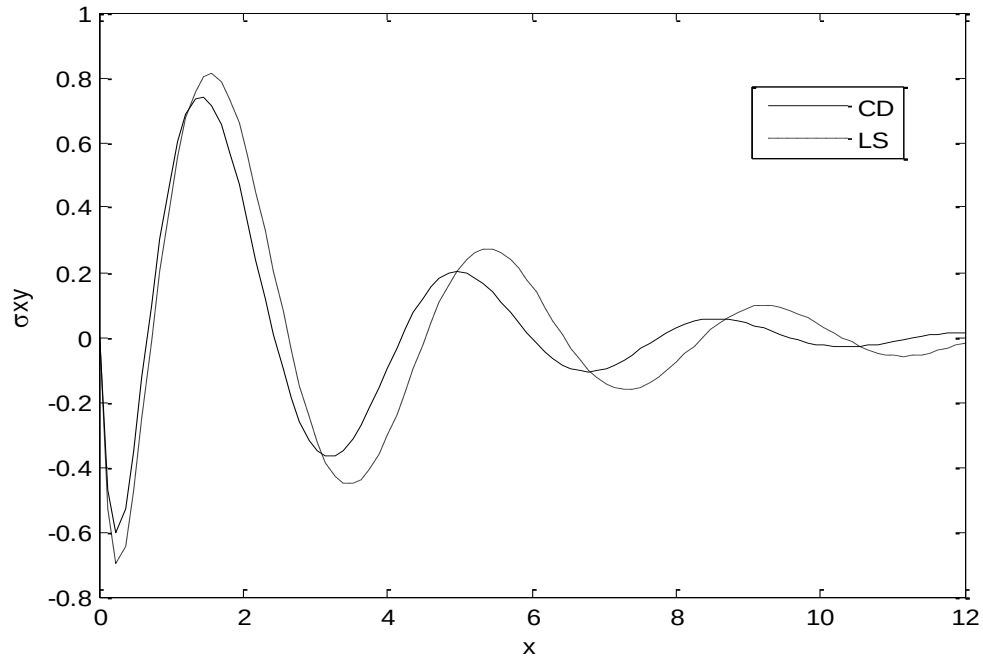

Figure 6. The distribution of stress component σ_{xy} for problem 1.

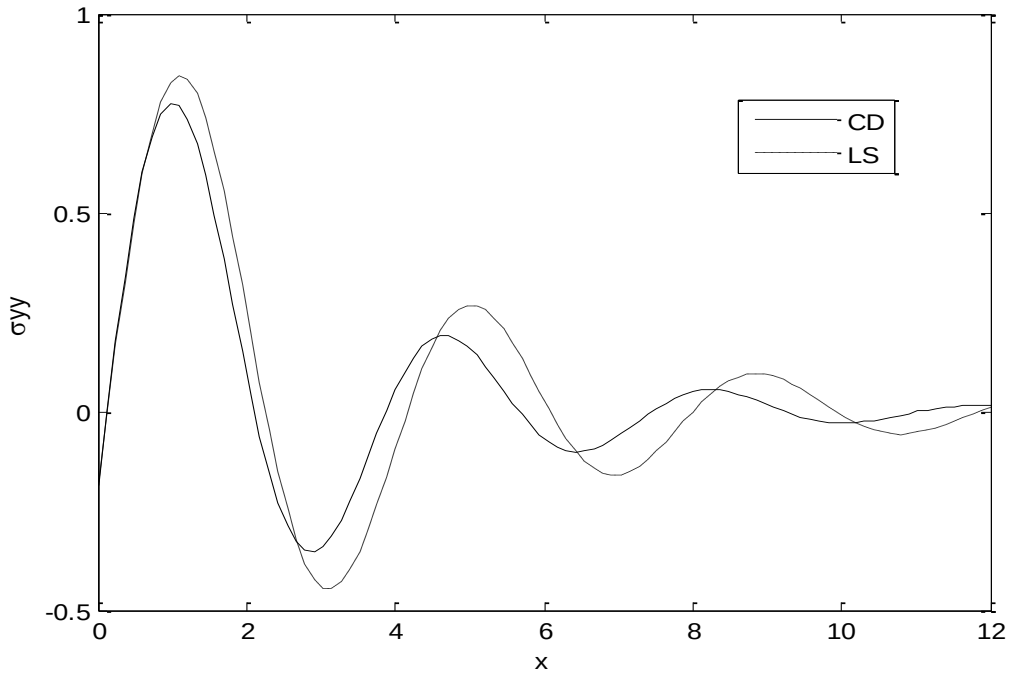

Figure 7. The distribution of stress component σ_{yy} for problem 1.

rises again to a maximum beyond about the crack end.

The stress component, σ_{xx} reach coincidence with negative value (Figure 5) and satisfy the boundary condition at $x=0$, reach the maximum value near the end of crack ($x \approx 1.2$) and converges to zero with increasing the distance x, also Figure 7 (satisfy the

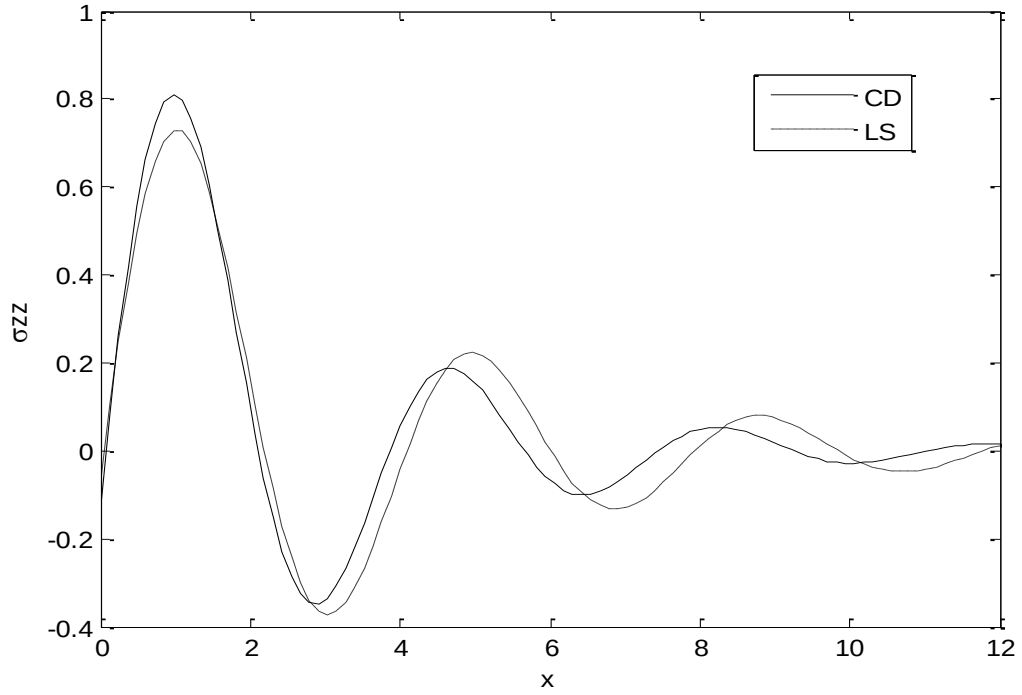

Figure 8. The distribution of stress component σ_{zz} for problem 1.

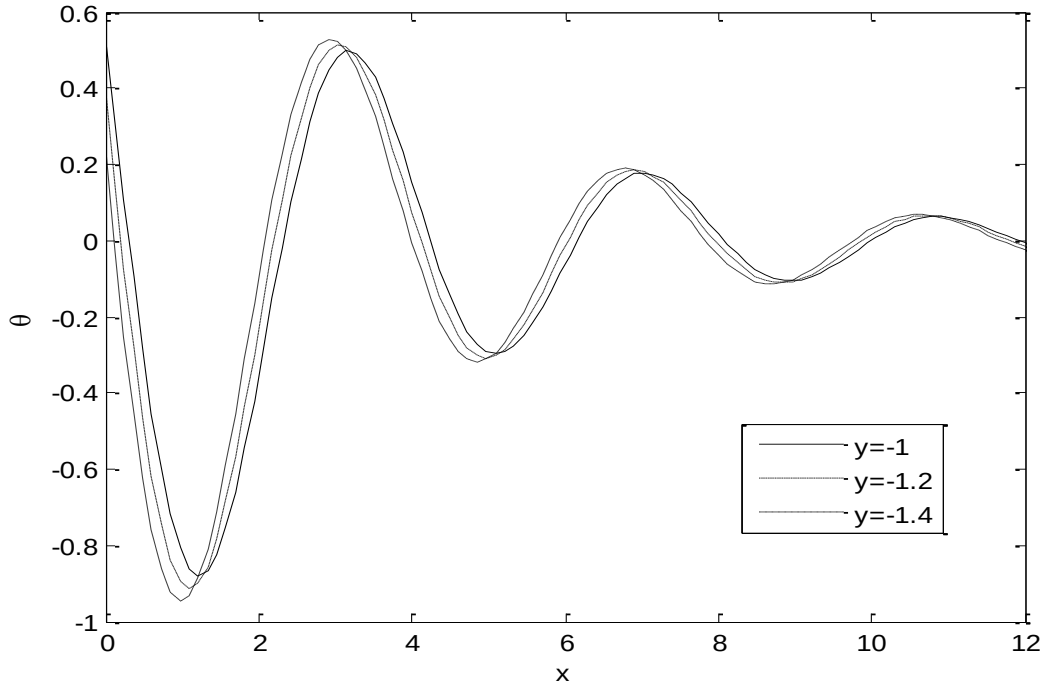

Figure 9. Temperature distribution with Variation of distances under LS theory (problem 1).

boundary condition at $x=0$) and 7, take the same behavior of Figure 5. Figure 6, shows that the stress component σ_{xy} satisfies the boundary condition at $x=0$ and had a different behaviour. It decreases in the start and start increases (maximum) in the context of the two theories until reaching the crack end. These trends

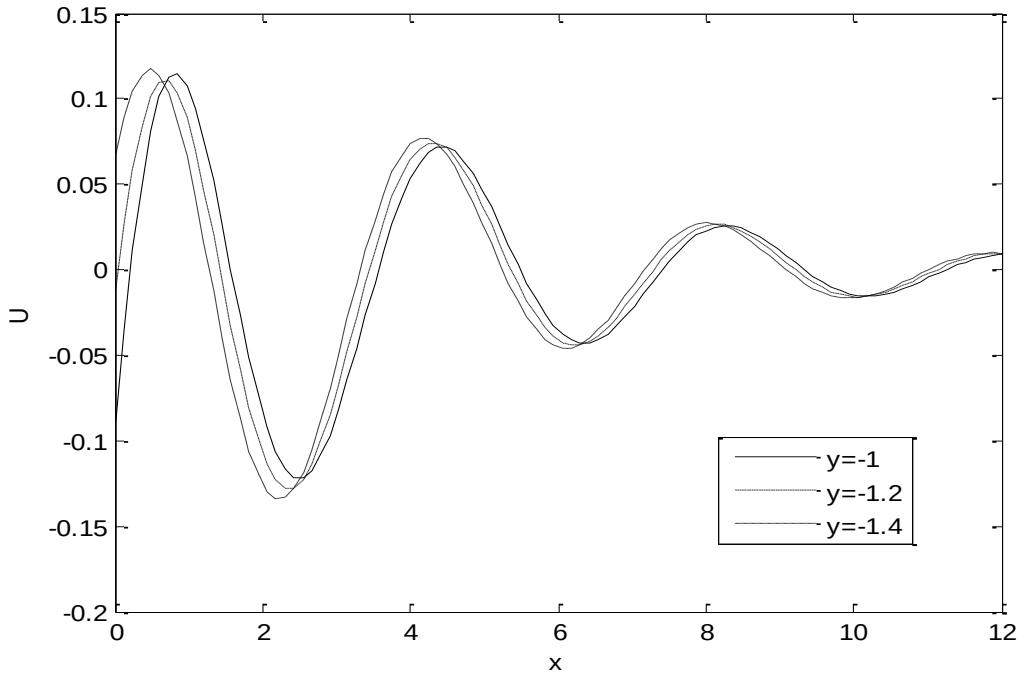

Figure 10. Displacement distribution u with variation of distance under L-S theory(problem 1).

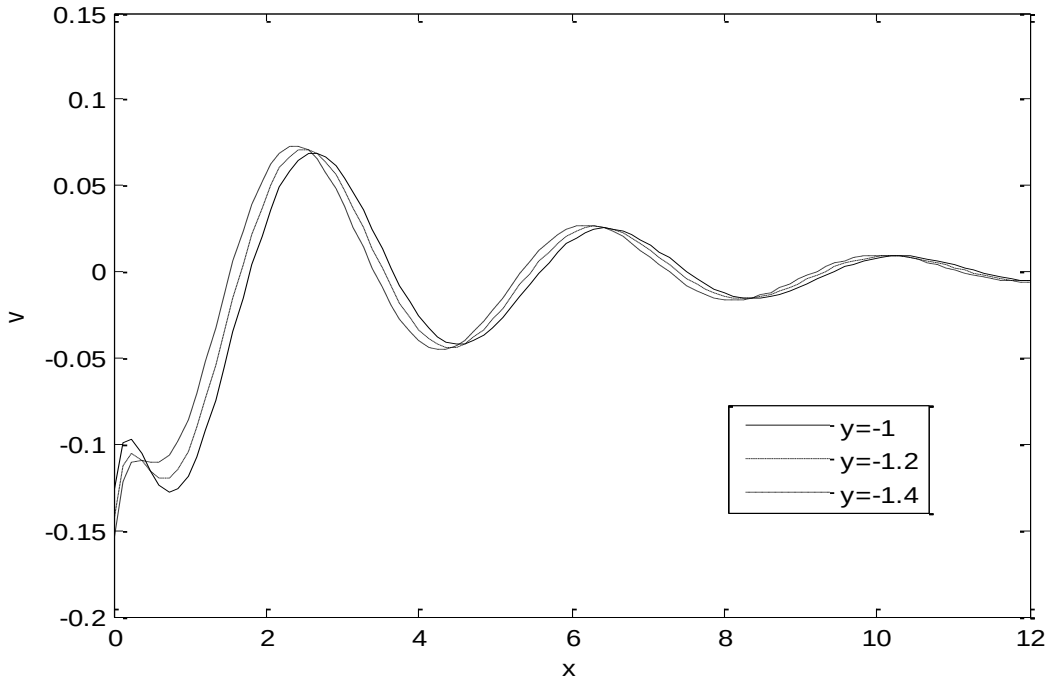

Figure 11. Displacement distribution v with variation of distance under LS theory(problem 1).

obey elastic and thermoelastic properties of the solid under investigation.

Figure 9-14 show the comparison between the temperature θ, displacement components u, v , the force stresses components σ_{xx} , σ_{yy} σ_{zz} and σ_{xz} , the case of different three values of y, (namely y= -1, y=-1.2 and y=-1.4) under (LS) theory. It should be noted (Figure 9) that in this problem. It is clear from the graph that θ

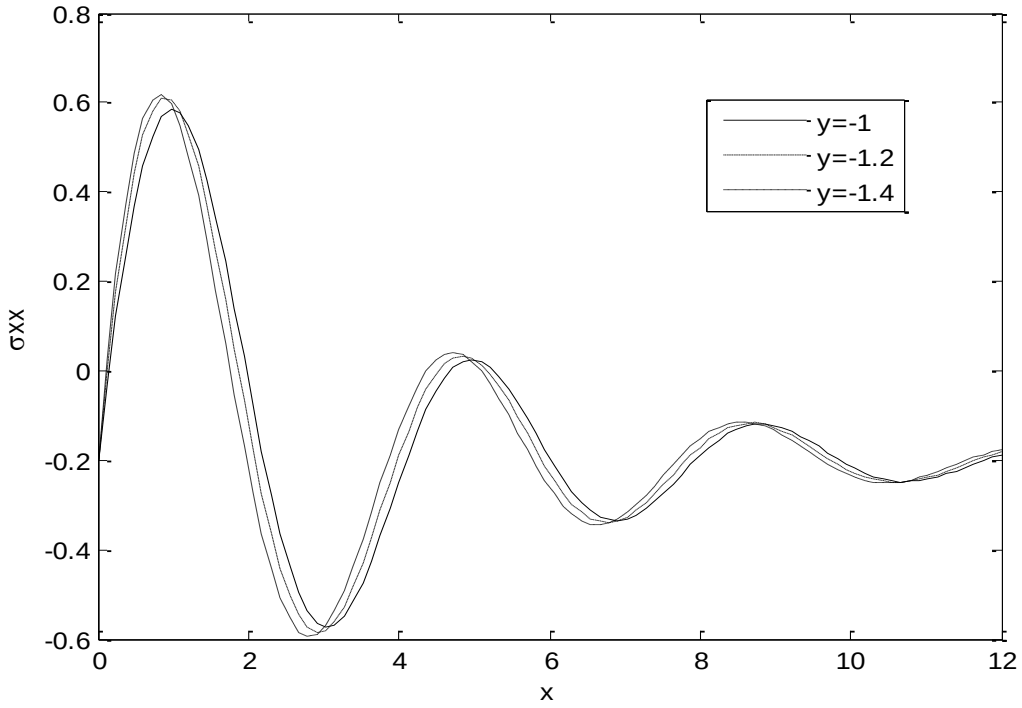

Figure 12. Stress distribution σ_{xx} with variation of distance under LS theory(problem 1).

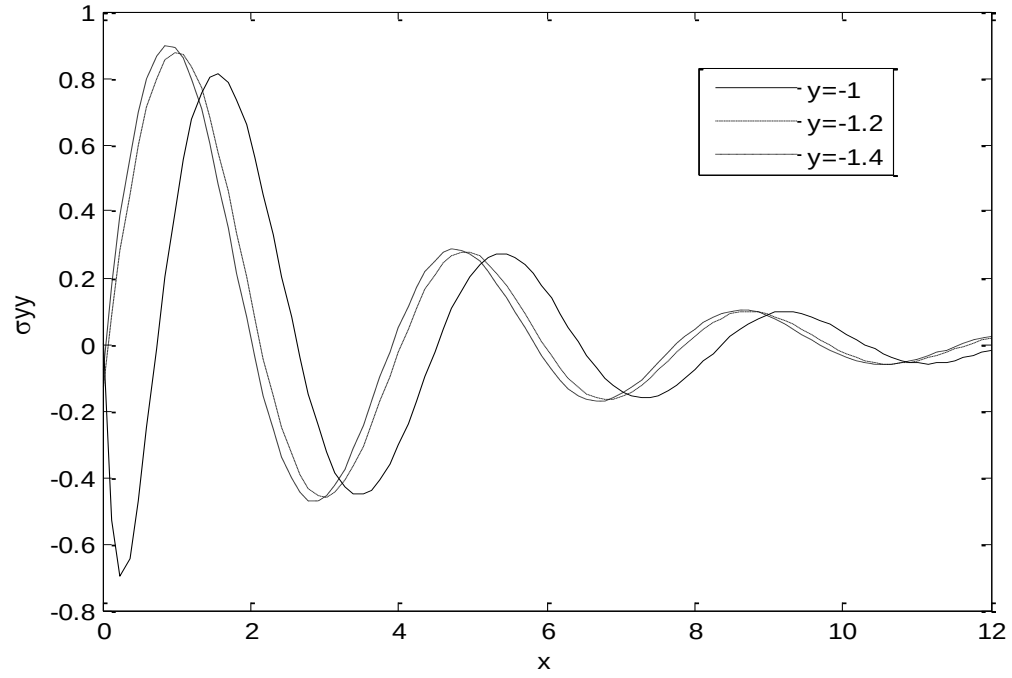

Figure 13. Stress distribution σ_{yy} with Variation of distance under LS theory (problem 1).

has minimum value at the beginning of the crack ($x=0$), it begins to fall just near the crack edge ($x\approx1.2$), where it experiences sharp increases (with maximum positive gradient at the crack's end). Graph

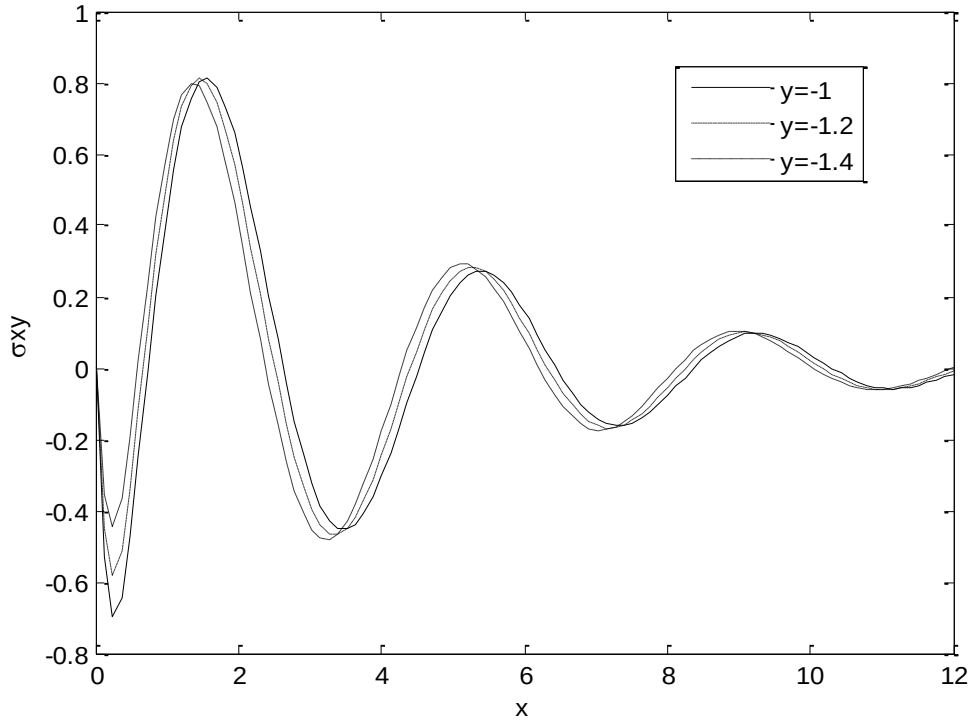

Figure 14. Stress distribution σ_{xy} with variation of distance under LS theory(problem 1).

lines for both values of y show different slopes at crack ends according to y-values. In other words, the temperature line for y =- 1 has the highest gradient when compared with that of y = -1.2 and y= -1.4 at the first of the range. In addition, all lines begin to coincide when the horizontal distance x is beyond the three double of the crack size to reach the reference temperature of the solid. These results obey physical reality for the behaviour of fiber as a polycrystalline solid.

Figure 10 the horizontal displacement u, despite the peaks (for different vertical distances y= -1, y=-1.2 and y=-1.4) occur at equal value of x, the magnitude of the maximum displacement peak strongly depends on the vertical distance y. it is also clear that the rate of change of u decreases with increasing y as we go farther apart from the crack. On the other hand, Figure 11 shows atonable increase of the vertical displacement v, near the crack end to reach minimum value beyond $x \approx 1.2$ reaching zero at the three double of the crack size (state of particles equilibrium). Figure 12, the horizontal stresses σ_{xx} Graph lines for both values of y show different slopes at crack ends according to y-values. In other words, the σ_{xx} component line for y = -1.4 has the highest gradient when compared with that of y = -1.2 and y= -1.4 at the edge of the crack. In addition, all lines begin to coincide when the horizontal distance x is beyond the three double of the crack size to reach zero after their relaxations at infinity. Variation of y has a serious effect on both magnitudes of mechanical stresses. These trends obey elastic and thermoelastic properties of the solid under investigation.

Figure 13, shows that the stress component σ_{yy} ,satisfy the boundary condition at $x = 0$, the line for y = -1.4 has the highest gradient when compared with that of y= -1 and y= -1.2 in the range $0 \le x \le 1.6$ (near the crack edge), the line for y = -1 has the highest gradient when compared with that of y=-1.2 and y=-1.4 in the range (near the crack end) $1.6 \le x \le 3$ and converge to zero when $x > 12$. These trends obey elastic and thermoelastic properties of the solid. Figure 14, shows that the stress component σ_{xy} satisfy the boundary condition, it decreases in the start and start increases (maximum) in the context of the three values of y until reaching the crack end, the line for y=-1.4 has the highest gradient when compared with that of y=-1.2 and y=-1 in the range $0 \le x \le 1.7$, the line for y=-1 has the highest gradient when compared with that of y=-1.2 and y=-1.4 in the range $1.7 \le x \le 3.5$ and converge to zero when $x > 12$. These trends obey elastic and thermoelastic properties of the solid.

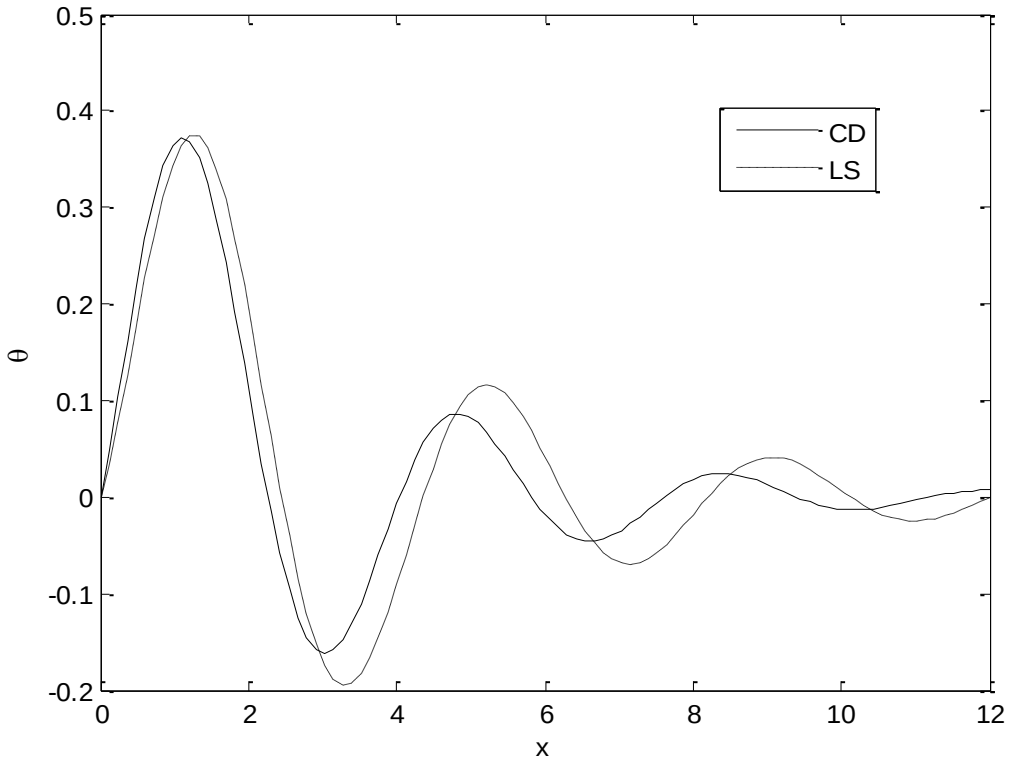

Figure 15. The temperature distribution for problem 2.

Problem 2

Figure 15 described the values of temperature θ under two theories. It indicts that the values of temperature θ increasing in the ranges $0 \le x \le 1.7$ and $3.2 \le x \le 5.2$ with fibre-reinforced and then decreases in the ranges $1.7 \le x \le 3.2$ and $5.2 \le x \le 6.5$. The values of temperature θ converge to zero with increasing the distance x.

In Figure 16, the horizontal displacement, u, begins with sharp decreases near the ($x \approx 1.4$), then smooth increases again to reach it's a maximum value just at near $x \approx 2.8$. Beyond it u falls again to try to retain zero at infinity. In Figure 17, the vertical displacement v, we see that the displacement component v always starts from the positive value and terminates at the zero value at the infinity (state of particles equilibrium). The displacements u and v show different behaviours, because of the elasticity of the solid tends to resist vertical displacements in the problem under investigation. Both of the components show different behaviours.

In Figure 18 the stress component, σ_{xx} reach coincidence with negative value and satisfy the boundary condition at $x = 0$, reach the maximum value near ($x \approx 3.3$) and converges to zero with increasing the distance x, also Figures 19-21 take the same behavior.

Figure 19, shows that the stress component σ_{xy} satisfy the boundary condition at $x = 0$ and had a different behaviour. It sharp increases in the start and start decreases (minimum) in the context of the two theories until reaching the crack end. These trends obey elastic and thermoelastic properties of the solid under investigation.

Conclusions

In the present study, the normal mode analysis is used to study the effect of the cracks of the problem under consideration at the free surface of a fiber-reinforced thermoelastic half-space based on the CD and L-S theory of thermoelasticity. According to the analysis above, we can conclude the following points:

(1) The curves in the context of the (CD) and (L-S) theories decrease exponentially with increasing x, this indicate that the thermoelastic waves are unattenuated and non dispersive, where purely thermoelastic waves undergo both attenuation and dispersion.

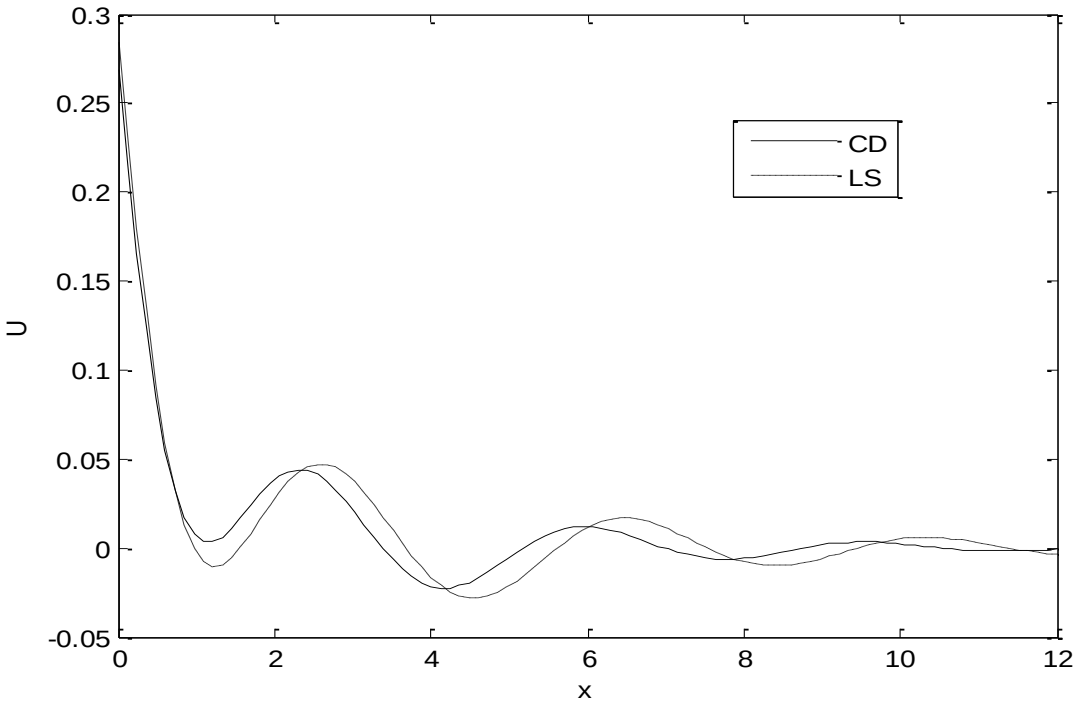

Figure 16. Horizontal displacement distribution u for problem 2.

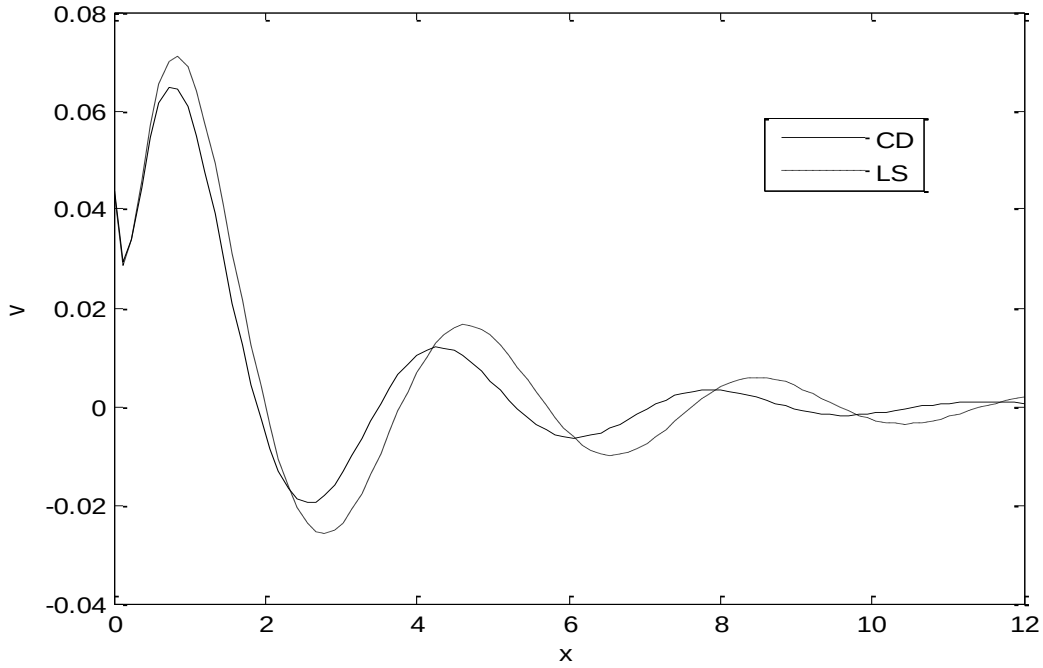

Figure 17. Vertical displacement distribution v for problem 2.

(2) The curves of the physical quantities with (CD) theory in most of figures are lower in comparison with those under (L-S) theory, due to the relaxation times.

(3) Analytical solutions based upon normal mode analysis for themoelastic problem in solids have been developed and utilized.

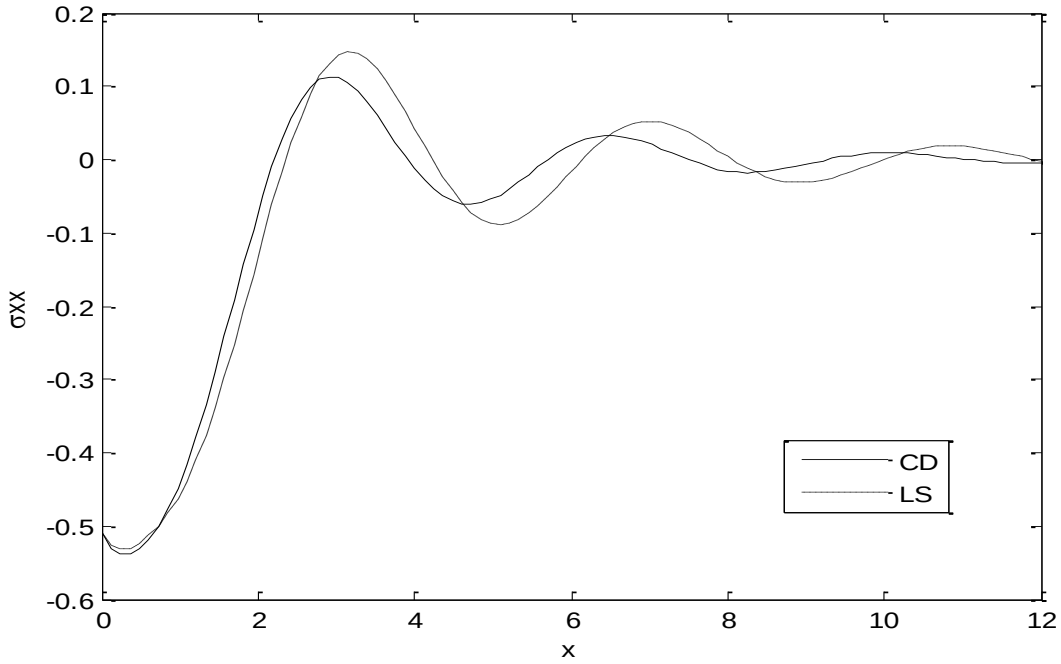

Figure 18. The distribution of stress component σ_{xx} for problem 2.

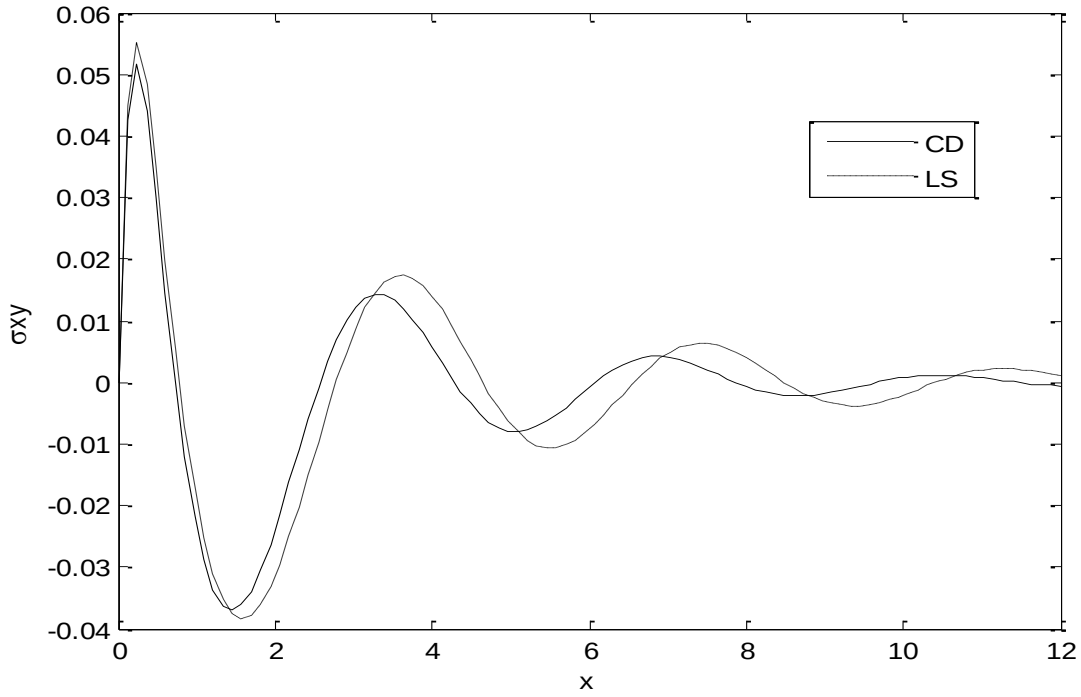

Figure 19. The distribution of stress component σ_{xy} for different problem 2.

(4) A linear opening mode-I crack has been investigated and studied for copper solid.

(5) Temperature, radial and axial distributions were estimated at different distances from the crack edge.

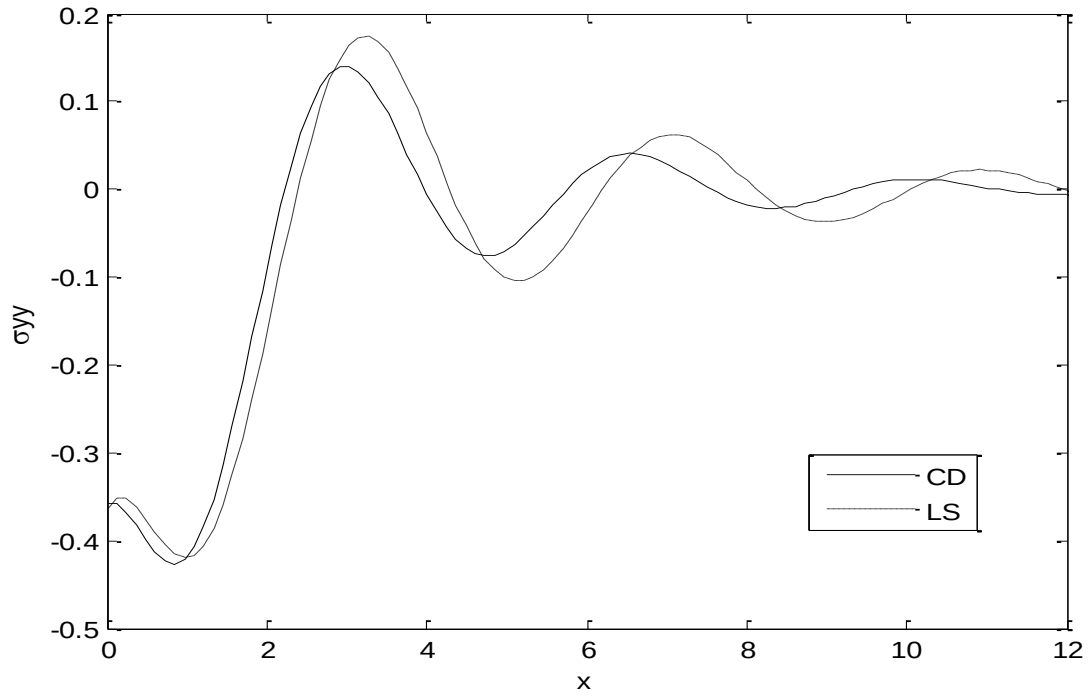

Figure 20. The distribution of stress component σ_{yy} for different problem 2.

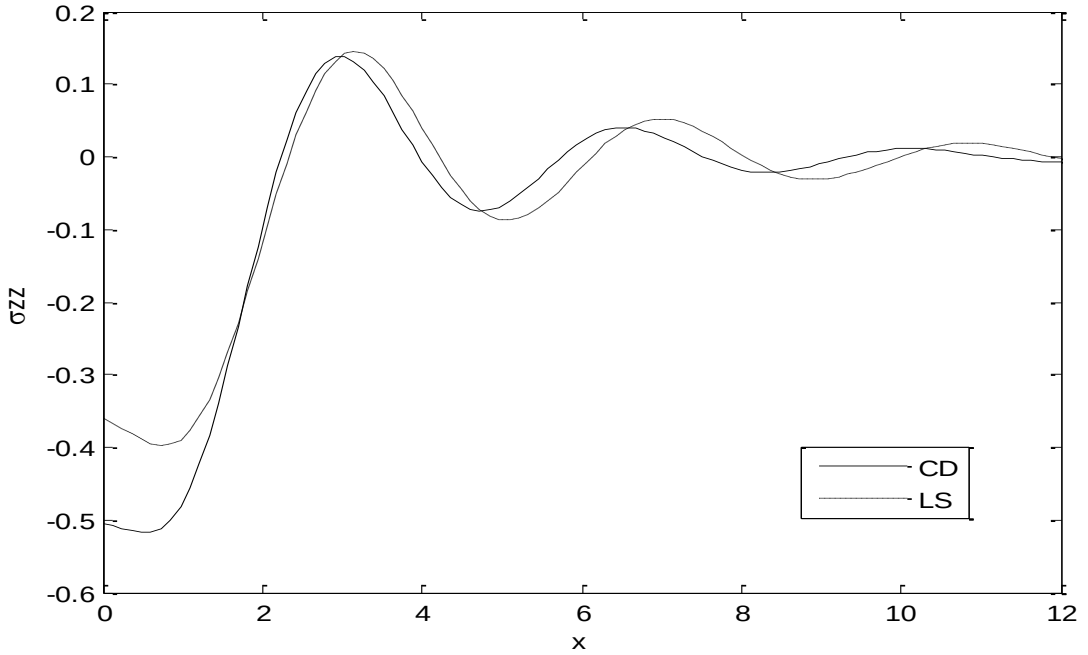

Figure 21. The distribution of stress component σ_{zz} for problem 2.

(6) The stresses distributions, and temperature were evaluated as functions of the distance from the crack edge.

(7) Crack dimensions are significant to elucidate the mechanical structure of the solid.

(8) Cracks are stationary and external stress is demanded

to propagate such cracks.
(9) It can be concluded that a change of volume is attended by a change of the temperature while the effect of the deformation upon the temperature distribution is the subject of the theory of thermoelasticity.
(10) The value of all the physical quantities converges to zero with an increase in distance y and All functions are continuous.
(11) The fibre-reinforced has an important role on the distribution of the field quantities.
(12) The method which used in the present article is applicable to a wide range of problems in thermodynamics and thermoelasticity.
(13) Deformation of a body depends on the nature of the applied force as well as the type of boundary conditions
(14) It is clear from all the figures that all the distributions considered have a non-zero value only in a bounded region of the half-space. Out side of this region, the values vanish identically and this means that the region has not felt thermal disturbance yet.
(15) The results presented in this paper should prove useful for researchers in material science, designers of new materials, low temperature physicists, as well as for those working on the development of a theory of hyperbolic thermoelasticity. The introduction of the crack to the generalized fiber-reinforced thermoelastic medium provides a more realistic model for these studies.

REFERENCES

Belfield AJ, Rogers TG, Spencer AJM (1983). Stress in elastic plates reinforced by fiber lying in concentric circles, J. Mech. Phys. Solids, 31:25-54.

Chattopadhyay A, Choudhury S (1990). Propagation, reflection and transmission of magneto-elastic shear waves in a self-reinforced medium, Int. J. Eng. Sci. 28:485-495.

Chattopadhyay A, Choudhury S (1995). Magnetoelastic shear waves in an infinite self-rein-forced plate, Int. J. Num. Anal. Methods Geomech. 19:289-304.

Chattopadhyay A, Venkateswarlu RLK, Saha S (2002). Reflection of quasi-P and quasi-SV waves at the free and rigid boundaries of a fibre-reinforced medium, Sãdhanã, 27:613-630.

Chaudhary S, Kaushik VP, Tomar SK (2004). Reflection/transmission of plane wave through a self-reinforced elastic layer between two half-spaces, Acta Geophysica Polonica. 52:219-235.

Dhaliwal R (1980). External Crack due to Thermal Effects in an Infinite Elastic Solid with a Cylindrical Inclusion. Thermal Stresses in Server Environments Plenum Press, New York and London, pp. 665-692.

Elfalaky A, Abdel-Halim AA (2006). A Mode-I Crack Problem for an Infinite Space in Thermoelasticity, J. Appl. Sci. 6:598-606.

Green AE, Lindsay KA (1972). Thermoelasticity. J. Elasticity 2:1-7.

Hasanyan D, Librescu L, Qin Z, Young R (2005). Thermoelastic Cracked Plates Carrying nonstationary Electrical Current. J. Thermal Stresses, 28:729-745.

Hashin Z, Rosen WB (1964). The elastic moduli of fibre-reinforced materials, J. Appl. Mech. 31:223-232.

Lord HW, Şhulman YA (1967). Generalized dynamical theory of thennoelasticity. J. Mech. Phys. Solid, 15:299-306.

Lotfy KH (2012a). Mode-I crack in a two-dimensional fibre-reinforced generalized thermoelastic problem, Chin. Phys. B, 21:1-014209.

Lotfy KH (2012b). The effect of a magnetic field on a 2D problem of fibre-reinforced thermoelasticity rotation under three theories, Chin. Phys. B; 21:6- 064214

Othman M, Atwa S (2012). Generalized Magneto-thermoelasticity in a Fibre- reinforced Anisotropic Half-space with Energy Dissipation, Int. J. Thermophys. 33(6):1126-1142.

Othman M, Lotfy KH (2009a). Effect of Magnetic Field and Inclined Load in Micropolar Thermoelastic Medium Possessing Cubic Symmetry, Int. J. Ind. Math. 1(2):87-104.

Othman M, Lotfy KH (2009b). Two-dimensional Problem of Generalized Magneto-thermoelasticity under the Effect of Temperature Dependent Properties for Different Theories, MMMS, 5:235-242.

Othman M, Lotfy KH (2010a). Generalized Thermo-microstretch Elastic Medium with Temperature Dependent Properties for Different Theories, Engineering Analysis with Boundary Elements, 34:229-237.

Othman M, Lotfy KH (2010b). On the Plane Waves in Generalized Thermo-microstretch Elastic Half-space, International Communication in Heat and Mass Transfer, 37:192-200.

Othman M, Lotfy KH (2013). The effect of magnetic field and rotation of the 2-D problem of a fiber-reinforced thermoelastic under three theories with influence of gravity, Mech. Mater. 60:120-143.

Othman M, Lotfy KH, Farouk RM (2009). Transient Disturbance in a Half-space under Generalized Magneto-thermoelasticity due to Moving Internal Heat Source, Acta Physica Polonica A, 116:186-192.

Othman M, Saied S (2012a). The Effect of Mechanical Force on Generalized Thermoelasticity in a Fiber-reinforced under Three Theories, Int. J. Thermophys. 33(6):1082-1099.

Othman M, Saied S (2012b). The Effect of Rotation on Two-dimensional Problem of a Fibre-reinforced Thermoelastic with One Relaxation Time, Int. J. Thermophys. 33(2):160-171.

Othman M, Saied S (2013). Two-Dimensional Problem of Thermally Conducting Fiber-reinforced under Green-Naghdi Theory, J. Thermoelasticity. 1 (1):13-20

Othman MIA, Song YQ (2007). Reflection of plane waves from an elastic solid half-space under hydrostatic initial stress without energy dissipation, Int. J. Sol. Struct. 44:5651-5664.

Pradhan A, Samal SK, Mahanti NC (2003). "Influence of anisotropy on the love waves in a self- reinforced medium", Tamkang J. Sci. Eng. 6(3):173-178.

Sengupta PR, Nath S (2001). Surface waves in fibre-reinforced anisotropic elastic media, Sãdhanã, 26:363-370.

Singh B (2006). Wave propagation in thermally conducting linear fibre-reinforced composite materials, Arch. Appl. Mech.75:513-520.

Singh B, Singh SJ (2004). "Reflection of planes waves at the free surface of a fibre- reinforced elastic half-space", Sãdhanã, 29:249-257.

Singh SJ (2002). Comments on "Surface waves in fibre-reinforced anisotropic elastic media" by Sengupta and Nath [Sãdhanã, 2001 26, 363-370]. Sãdhanã. 27:1-3.

Ueda S (2003). Thermally induced fracture of a piezoelectric Laminate with a crack Normal to Interfaces, J. Thermal Stresses, 26:311-323.

Verma PDS (1986). Magnetoelastic shear waves in self-reinforced bodies, Int. J. Eng. Sci. 24:1067-1073.

Verma PDS, Rana OH, Verma M (1988). Magnetoelastic transverse surfaces waves in self-reinforced elastic bodies, Ind. J. Pure Appl. Math. 19:713-716.